FORUM GEOGRAFI
ISSN: 0852-0682 | E-ISSN: 2460-3945

Estimation of Sea Surface Salinity Concentration from Landsat 8 OLI Data in the Strait of Madura, Indonesia

Muhsi Muhsi[1,*], Bangun Muljo Sukojo[2], Muhammad Taufik[2], Pujo Aji[2], Lalu Muhamad Jaelani[2]

[1] Faculty of Engineering, Universitas Islam Madura, Pamekasan, Indonesia
[2] Faculty of Civil, Planning, and Geo Engineering, Institut Teknologi Sepuluh Nopember, Surabaya, Indonesia

[*)] Correspondence: muhsi@uim.ac.id

Citation:
Muhsi, M., Sukojo, B.M. , Taufik, M., Aji, P., & Jaelani, L.M. (2022) Estimation of Sea Surface Salinity Concentration from Landsat 8 OLI Data in the Strait of Madura, Indonesia. Forum Geografi. Vol. 36, No. 2.

Article history:
Received: 02 October 2022
Accepted: 28 December 2022
Published: 28 December 2022

Abstract

Remote sensing technique to estimate the sea surface salinity has been widely implemented in the seas of various regions. The interface between them was developed using a regression equation like the algorithm in previous research. However, the use of this algorithm for waters in Indonesia, especially in Madura Strait, still requires some adjustment since it is related to the characteristics of different areas in which the algorithm was developed. The development of an applicable local algorithm was performed by finding the best coefficient value in estimating sea surface salinity by considering the value of its lowest NMAE (Normalized Mean Absolute Error). By using salinity and in-situ Rrs(λ) (Reflectance of remote sensing) data, we found that the coefficient for the slope was -0.0092, and the intercept was 1.4903. The developed algorithm produces higher accuracy than the existing algorithm, with an NMAE of 0.51%. This NMAE value is smaller than previous research, so this new model can be used to estimate sea surface salinity, particularly in Indonesian sea waters.

Keywords: Estimation, Sea Surface Salinity, Landsat 8, Madura Strait

1. Introduction

Salinity in seawater has an important role in the evolution of seawater microbial organisms, such as macroalgae or seaweeds, and other organisms living in the same place (Akhter *et al*., 2021; Lobban & Harrison, 1997). This phenomenon can occur since salinity affects the osmoregulation process in aquatic plants (Abe *et al*., 2021; Nybakken, 2001). In addition, salinity can indicate whether seawater can be used in salt production (Cuthbert *et al*., 2021; Nafizah *et al*., 2016). Thus, the information on salinity concentration becomes important for salt farmers and for planning the development of seaweed farming.

Currently, there are two methods for measuring the concentration of seawater the in-situ method, a method of estimating the salinity by directly measuring it on the sea as well as by collecting seawater samples and then measuring it in the laboratory, and the indirect method, the estimation of seawater salinity by using remote sensing data (Budhiman, 2012; Scale, 2009; Wang & Xu, 2008). However, by considering water bodies' spatial and temporal heterogeneity, extracting water information by remote sensing techniques can be more effective than an *in-situ* field measurement (Liu *et al*., 2003). Sea surface salinity (SSS) concentration could be retrieved by analyzing satellite images without direct contact with the object (George, 2005; Lillesand *et al*., 2004).

SSS retrieval from satellite images strongly depends on the surface reflectance accuracy produced through the atmospheric correction algorithm and parameter retrieval algorithm (Jaelani *et al*., 2015, 2016; Jaelani *et al*., 2013). Currently, several existing SSS retrieval algorithms have been developed and frequently used by researchers (Nafizah *et al*., 2016), such as the algorithm of Young Baek Son (Son *et al*., 2012), Wouthuyzen Sam (Wouthuyzen *et al*., 2008), Ahn YH (Ahn. *et al*., 2008), Yan Bai (Bai *et al*., 2013), Hiroaki Sasaki (Sasaki *et al*., 2008) and Binding (Binding & Bowers, 2003). Because SSS algorithms are site-specific and time-dependent, This existing algorithm which is mainly developed and tested in water areas outside Indonesian waters may be affected by the characteristics from the location and pollutant aspects that are possibly different. Therefore, this study aims to validate the existing algorithm's performance and develop a new suitable one for the geographical conditions of the waters in Indonesia, especially in Madura Strait (Muhsi *et al*., 2017, 2018, 2020).

2. Research Methods

2.1. Study area

The study area was at Madura Strait of East Java Province, Indonesia. It is located between 07° 08' 30"S - 07° 44' 27"S Latitude and 112° 39' 23"E - 114° 05' 24"E Longitude (Figure 1); between two islands, i.e. Java and Madura. Madura Strait, in the north side of it, is bordered by four regencies: Bangkalan, Sampang and Sumenep, and Pamekasan, respectively. Over the past few years, the waters in the Strait of Madura have been used as raw materials for producing salt and as seaweed farmland. According to data from the Ministry of Marine Affairs and Fisheries of the Republic of Indonesia, for a national salt production run by PT. Garam company, Madura has

contributed 17% of total production of 19201.9 tons-per-August 2017. Thus, it is crucial to know and map the sea surface salinity in Madura strait as consideration of decision-making in various interests, especially salt and seaweed farming.

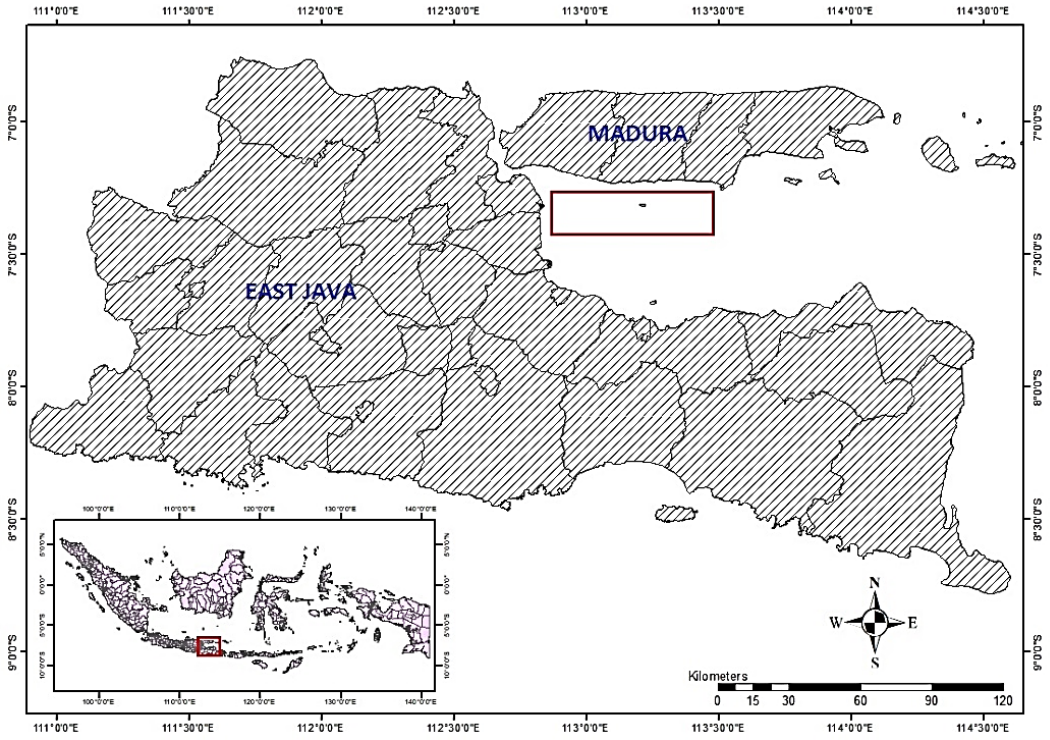

Figure 1. Study area.

2.2. Data collection

Field data was taken in Madura strait waters, consisting of SSS data (collected by a refractometer) and *in-situ* Rrs(λ) (indirectly recorded by a Spectroradiometer). The field campaign and acquisition of Landsat 8 data were performed on June 2, 2016. From that field survey, there were 20 SSS data as well as apparent optical properties of water (AOP), such as upward radiance (L_u), downward radiance atmosphere (L_s), and downward irradiance atmosphere (E_d). Since the Rrs(λ) value cannot be directly measured in the field (Mobley, 1999b), it was calculated by using the equation of Gordon and Mobley (Gordon *et al.*, 1988; Mobley, 1999b) in (Budhiman, 2012). The sampling locations, both SSS and AOP, are at the same coordinates to avoid bias. The flow chart of this research process is shown in Figure 2.

2.3. Insitu data processing

The AOP data was measured using spectroradiometer Tri-OS RAMSES with a wavelength range of 320–950nm and intervals of approximately 3.3nm. Tri-OS RAMSES used is a hyperspectral spectroradiometer that was fitted into Landsat 8 OLI bands: Band 1 (433nm-453nm), Band 2 (450nm-515nm), Band 3 (525nm-600nm), Band 4 (630nm-680nm) dan Band 5 (845nm-885nm). Measurements were taken on June 2, 2016. Equation 1 expresses the formula for calculating Rrs(λ) (Mobley, 1999b).

$$R_{rs}(\lambda) = \frac{L_w(\lambda)}{E_d(\lambda)} \quad (1)$$

$$L_w(\lambda) = L_u(\lambda) - \rho_s L_s(\lambda) \quad (2)$$

Equation 2 expresses water leaving radiance calculation, where Lw (water leaving radiance / Wm-2sr-1) is the radiance value obtained from the water column and radiance reflected directly by the thin layer of the sea surface (Nababan *et al.*, 2013), Ls (downward radiance atmosphere / Wm-2sr-1), ρs is a part of the reflectance on the surface of waters from reflected sunlight. ρs can be calculated using the Fresnel formula (Hecth *et al.*, 2002) (Budhiman *et al.*, 2012). ρs can also use the constant value of research results (Mobley, 1999a) or the constant value of 0.02 (Nababan *et al.*, 2013).

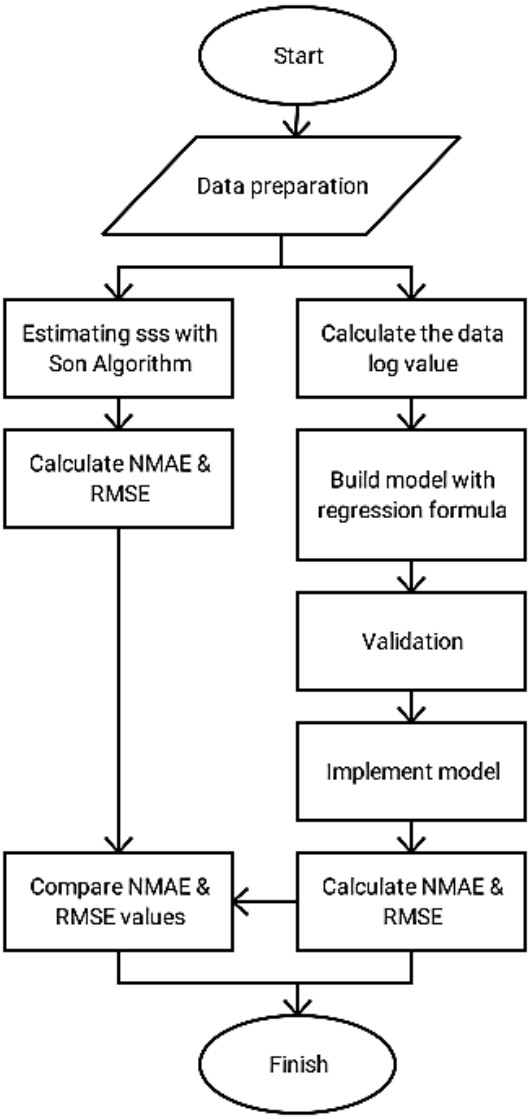

Figure 2. Flow diagram of the research process.

The first step in the calculation was started by calculating the diffuse attenuation coefficient (Kd) from a downward irradiance atmosphere (Ed). Kd is the coefficient for the propagation of light absorption by water column from the surface to the ocean depth (Lee & Carder, 2005a). Kd, also known as Cp (the surface water beam attenuation coefficient) by Son (Son *et al.*, 2012) is also very important for marine analysis, such as water class classification or light intensity in water depth (Lee *et al.*, 2002, 2005; Lee & Carder, 2005b; Wei & Lee, 2013a) Based on research conducted by Lee *at al.*, there are three methods for calculating the value of Kd. First, estimating the Kd at a wavelength of 490 by using an empirical algorithm; other Kd for the other wavelengths can be calculated afterward (Austin & Petzold, 1981, 1986; Lee & Carder, 2005). Second, using the value of chlorophyll-a. After the value of the first chlorophyll a is found, then it can be used to estimate the values of another Kd and chlorophyll-a (Lee & Carder, 2005b; Morel, 1988; Morel & Maritorena, 2001). Third, using a numerical simulation method of the flow movement of light in the sea (Lee & Carder, 2005b). The method was a semi-analytical calculation of Kd from Rrs(λ) calculated previously using Equation 1. However, the semi-analytical approach for determining Kd for each wavelength already considered the value of light absorption and backscattering as input coefficients. Therefore, this process uses the quasi-analytical method wherein the Rrs becomes its data input (Lee & Carder, 2005b; Wei & Lee, 2013b).

Meantime, Son YB calculates the value of Kd using the formula of maximum normalized difference carbon index (MNDCI) in developing the SSS algorithm (Son *et al.*, 2012). Son YB

determined the Kd value by using a multiple wave approach, assuming that when the particle concentration level increases, the peak radiance shifts to a longer wavelength band; in this case, he used the maximum normalized difference carbon index (MNDCI) formula. However, the multi-spectral MNDCI approach (Equation 3) was used for consideration that the values obtained would be more accurate than the wavelength ratio or single beam, particularly for waters containing a mixture of organic and inorganic components. Through the value of MNDCI, the Kd will be determined (Equation 4). This study used Son's formula to calculate the value of Kd since it will also be implemented to predict the sea surface salinity (Son *et al.*, 2012), especially in Madura Strait.

$$\text{MNDCI} = \frac{[nLw(555) - max(nLw(412), nLw(443), nLw(490))]}{[nLw(555) + max(nLw(412), nLw(443), nLw(490))]} \quad (3)$$

Where MNDCI is the maximum normalized difference carbon index, nLw is spectral normalized water-leaving radiance. While the *Kd* is determined using the following model (Son *et al.*, 2012) :

$$Kd = 10^{[0.70xMNDCI^3 + 0.96xMNDCI^2 + 1.14xMNDCI - 0.25]} \quad (4)$$

Where Kd is the attenuation coefficient, MNDCI is obtained from Equation 3. After the Kd for each wavelength has been obtained, the analysis will be done using Son's salinity algorithm (Son *et al*., 2012) (Equation 5).

$$SSS = 10^{[-0.141xlog_{10}(Kd) + 1.45]} \quad (5)$$

Where SSS is the sea surface salinity that would be predicted, and Kd is the attenuation coefficient obtained from Equation 4. SSS of Son algorithm results will be correlated with in-situ SSS data. Furthermore, the accuracy of the algorithm model will be tested using the Normalized Mean Absolute Error (NMAE) and Root Mean Square Error (RMSE) methods (Elkhrachy, 2021; Liemohn *et al*., 2021).

$$NMAE(100\%) = \frac{1}{N}\sum \left|\frac{x\ esti - x\ meas}{x\ meas}\right| \times 100 \quad (6)$$

Where NMAE is a value to see the average absolute error between the value of the SSS obtained from the measurement and in-situ, normalized by percentage *x esti* is in-situ SSS data and *x meas* is SSS data obtained from the model. At last, this algorithm model was then implemented using Landsat 8 data and validated using in-situ data. Finally, the RMSE is used to determine each data's standard deviation (Equation 7).

$$RMSE = \sqrt{\frac{\sum_{i=1}^{n}(X_{esti} - X_{meas})^2}{N}} \quad (7)$$

2.3. Satellite data processing

The data used to implement the prediction method was obtained from Landsat 8 OLI (path/row 118 and row 65) that is available for the public at https://earthexplorer.usgs.gov/ or http://glovis.usgs.gov/. The date of the image taken is the same as the date of field data collection, which is June 2, 2016.

Landsat 8 OLI images were taken in the Landsat Collection 1 Level-2 (On-Demand) directory, which is Landsat 8 OLI/TIRS C1 Level-2 data. In this case, to obtain the Rrs(λ) value of the sea surface on each pixel of Landsat 8 OLI images, the pixel value should be divided by 10000 to obtain the sea surface reflectance value. Then, the result will be divided by a constant value of phi (π) to obtain the Rrs(λ). Landsat 8 Operational Land Imager (OLI) surface reflectance products (Level-2) are generated using the Land Surface Reflectance Code (LaSRC) algorithm (Version 1.5.0), so no geometric correction is needed.

3. Results and Discussion

3.1. TriOS Ramses data and in-situ salinity correlation with the result of estimation

There was three data parameters were retrieved from in-situ AOP data collected using TriOS Ramses spectroradiometer, they were upward radiance (Lu), downward radiance atmosphere (Ls) and downward irradiance atmosphere (Ed), as shown in Figure 3. Furthermore, the following step is calculating Rrs(λ) value using Formula 1 and Formula 2, then MNDCI and Kd were calculated based onthe Rrs(λ) (Formula 3 and Formula 4). However, this study used only band 2 and band 3 since they accord with the ratio formula in MNDCI as shown in Table 1.

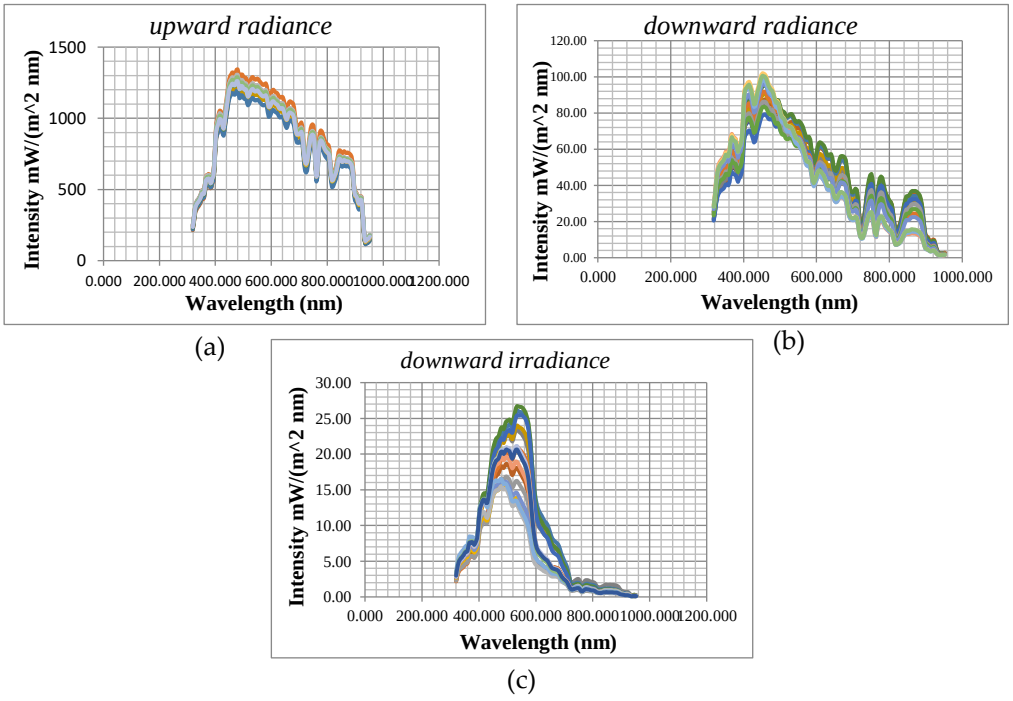

Figure 3. Graph of water upward radiance (a), downward atmosphere radiance (b), and downward irradiance (c).

Table 1. Rrs(λ), MNDCI, and Kd values.

Station	Rrs		MNDCI	Kd
	Band 2	Band 3		
2	0.016769	0.017564	0.023152	0.598552
4	0.018121	0.021336	0.081479	0.708418
6	0.016342	0.019711	0.093437	0.734883
8	0.011965	0.01083	-0.04978	0.495612
10	0.008756	0.005702	-0.21122	0.349746
12	0.011457	0.008881	-0.12668	0.415487
14	0.010555	0.007372	-0.17758	0.373676
16	0.011419	0.007939	-0.1798	0.37201
18	0.015111	0.014813	-0.00994	0.547882
20	0.019214	0.024202	0.114879	0.786342

Here, the Kd acts as an input value in Son algorithm to estimate the sea surface salinity. Based on the Kd in Table 1, two things can be obtained; first, salinity values which is in the form of particle salinity unit (PSU) as seen in Table 2. Second, a correlation graph between in-situ SSS values and the SSS values obtained from the estimation using the other algorithm, wherein the NMAE value is 3.4% and the RMSE value is 1.20 (see Figure 4).

Table 2. The *in-situ* and the estimation SSS with other algorithms.

Station	Sea Surface Salinity	
	In situ	**Estimation**
2	31.15	30.30
4	30.78	29.59
6	30.89	29.43
8	30.91	31.12
10	31.18	32.68
12	31.18	31.90
14	31.25	32.38
16	31.3	32.40
18	31.23	30.68
20	31.28	29.16

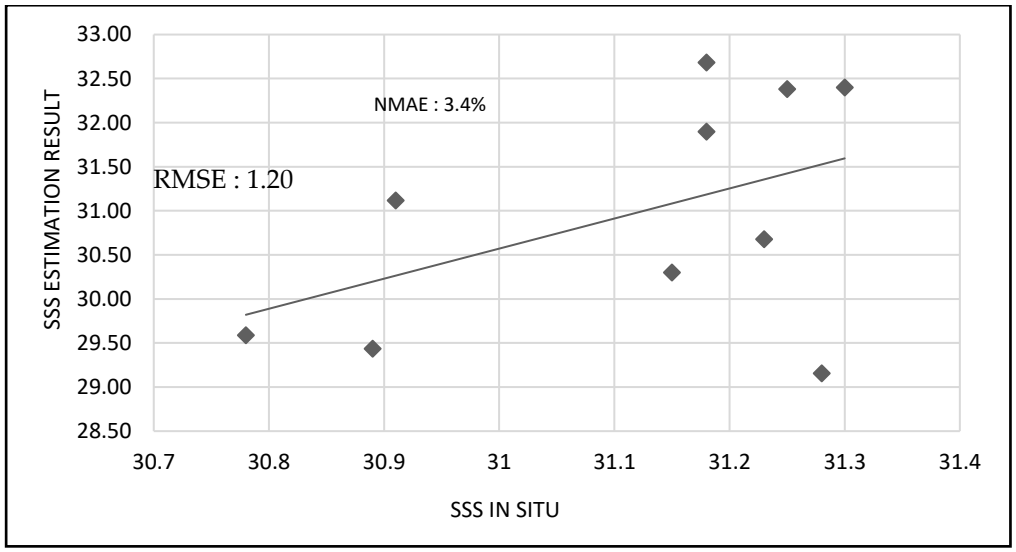

Figure 4. The correlation of the estimated and the *in-situ* SSS using other algorithms.

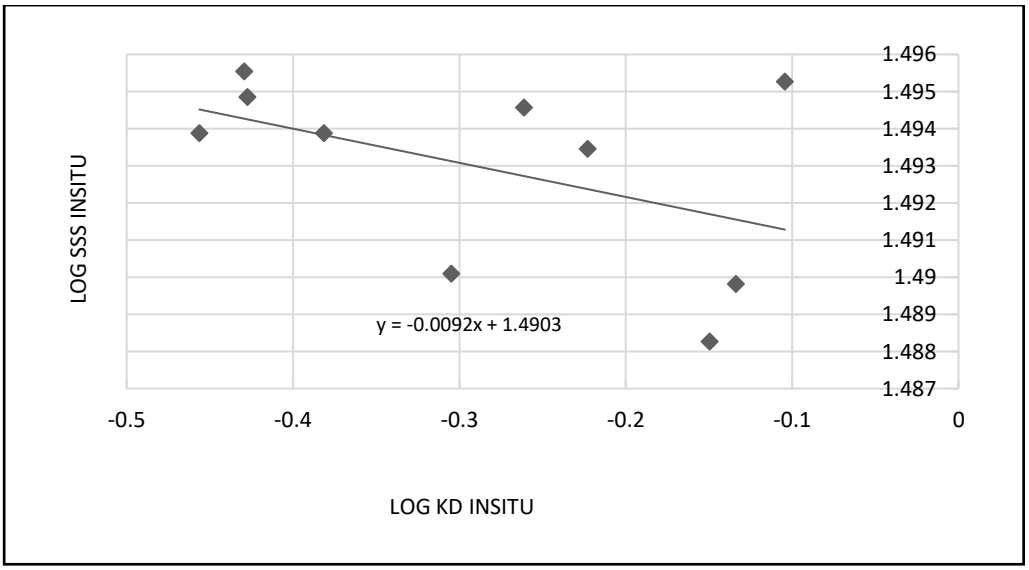

Figure 5. Graphical model of the developed algorithm.

3.2. Developed algorithm

The algorithm model was then developed using the regression model (Figure 5) and calculated using the Son algorithm method (Son *et al.*, 2012). From 20 SSS data taken, ten data were used to develop the algorithm model, and ten were used for validation. The algorithm will be used to estimate the sea surface salinity of Madura Strait (Equation 8).

$$SSS = 10^{[-0.0092\times(log_{10}(Kd))+1.4903]} \quad (8)$$

Where -0.0092 and 1.4903 were the coefficient and the constant, respectively, obtained from the development of the algorithm.

The result of the developed algorithm model was applied to different in-situ data with the data used previously when constructing the model. The estimation results of the SSS using the new algorithm model was shown in Table 3 and Figure 6.

Table 3. The in-situ and estimated SSS results with new algorithm.

Station	Sea Surface Salinity	
	In situ	**Estimation**
1	31.18	31.1
3	30.95	31.0
5	30.82	31.0
7	30.99	31.1
9	31.01	31.2
11	31.00	31.2
13	31.27	31.1
15	31.38	31.2
17	31.27	31.1
19	31.26	31.0

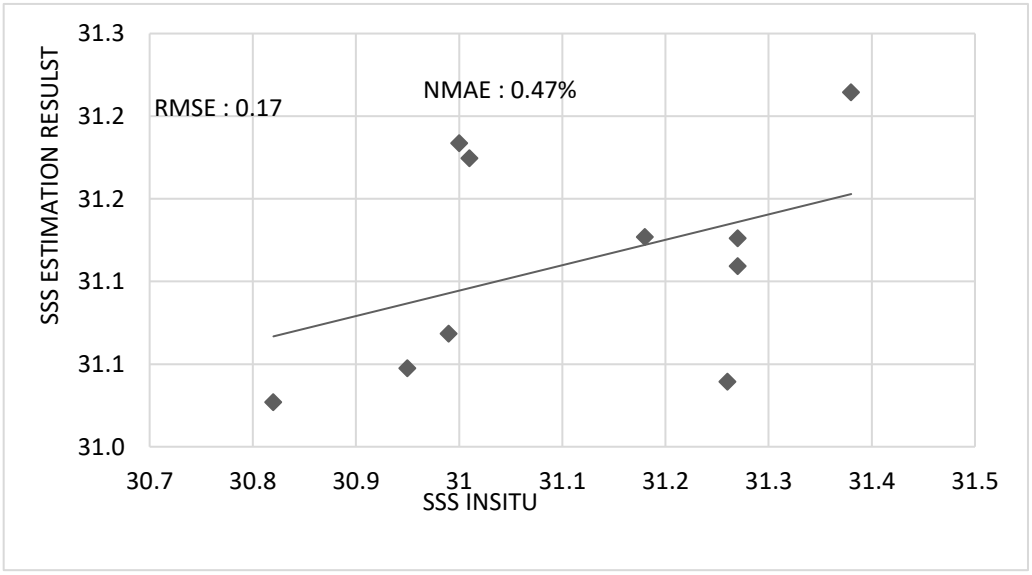

Figure 6. In-situ and estimated SSS correlation: new algorithm.

3.3. Validation

In this current study, validation was intended to test the validity of the new algorithm model (Formula 7) in estimating the sea surface salinity. Therefore, the validation method used Normalized Mean Absolute Error (NMAE) and Root Mean Square Error (RMSE) formula (Elkhrachy, 2021; Liemohn *et al.*, 2021) and as many as 10 data of SSS (Hair *et al.*, 2006) in the form of field measurement data.

The NMAE value was used to measure the validity of the algorithm. It is used to compare the SSS predicted value with the in-situ SSS, or to measure the absolute error of the SSS prediction model, which is in the form of a percentage. Further, the calculation results using the developed algorithm model were a very small NMAE value below 1%, i.e., 0.47%, and RMSE 0.17, as shown in Table 3 and Figure 5. Figure 5 shows that the value NMAE is 0.47% smaller than the NMAE of the other model, that is, 3.4% and RMSE 1.20 (Figure 3). This indicated that the developed algorithm

model is adequate to estimate the SSS value of Madura Strait. Whereas the smaller of RMSE value, the better.

3.4. Model implementation

The developed algorithm was then applied using Rrs(λ) of Landsat 8 OLI. The value then converted into Kd value using Son's formula (Son *et al*., 2012). The sea surface salinity in Madura strait water was then calculated based on that Kd using the previously developed algorithm model. Then also calculated using the other algorithm as a comparison. The comparison of the two salinity values obtained from Landsat 8 OLI and in-situ observation can be seen in Figure 7. and Table 4. In Figure 6 shows that the NMAE value of the new algorithm calculation is smaller, which is 0.51% and RMSE 0.19 (Figure 7(a)) compared to the value of NMAE from the other algorithm, which is 5.27% and RMSE 1.95 (Figure 7(b)).

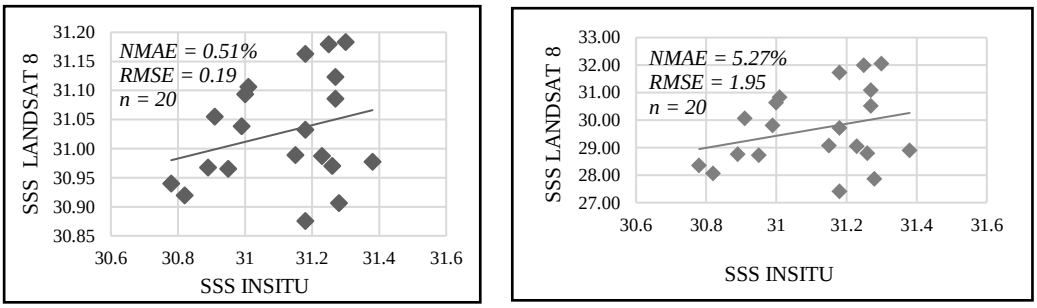

(a) **(b)**

Figure 7. The correlation of *in-situ* SSS and estimated SSS from Landsat 8 OLI ((a) calculated using the new algorithm, (b) calculated using the other algorithm.

Table 4. *In-situ* SSS and estimation SSS calculated with new algorithm and another algorithm to the Landsat 8 OLI images.

Station	Sea Surface Salinity		
	In situ	New Algorithm	Another Algorithm
1	31.18	30.88	27.42
2	31.15	30.99	29.08
3	30.95	30.97	28.73
4	30.78	30.94	28.36
5	30.82	30.92	28.06
6	30.89	30.97	28.77
7	30.99	31.04	29.82
8	30.91	31.06	30.07
9	31.01	31.11	30.84
10	31.18	31.16	31.73
11	31.00	31.09	30.64
12	31.18	31.03	29.72
13	31.27	31.09	30.53
14	31.25	31.18	31.99
15	31.38	30.98	28.91
16	31.3	31.18	32.06
17	31.27	31.12	31.10
18	31.23	30.99	29.06
19	31.26	30.97	28.81
20	31.28	30.91	27.87

Each seawater has characteristics consistent with environmental conditions, geography, and countries where it belongs (English *et al*., 1997; Salim *et al*., 2017). This affects the reflectance received in the satellite record sea surface. In this condition, the algorithms will also be influenced by the reflectance values (Rrs) that were used as independent variables in estimating and extracting element content in the seawater. As an algorithm created by Son to estimate the salinity of seawater is made using a case study in the Northeastern Gulf of Mexico (Son *et al*., 2012) will have a difference when applied in Indonesian waters. So, in this case, the algorithm with the Indonesian

waters' data base would have smaller NMAE and RMSE values. The distribution map of SSS in the Madura strait, recorded on June 2, 2016, is shown in Figure 8.

This study has an advantage because the reflectance value used is in situ. However, it has limitations from the data aspect. In further research, additional data is needed so that it is possible to have better accuracy. In addition, since the SSS estimate method presently only employs the reflectance value, it can be improved by experimenting with data mining techniques, which need more than one attribute. For example, attributes that might be used are sulfate, sea surface temperature, total suspended soil, or chlorophyll-a. However, all of that can still be estimated using remote sensing techniques so that in the use of image data, one is sufficient to extract all these attributes. Meanwhile, data mining techniques that may be used are estimation or forecasting using algorithms such as Neural Network (NN), Linear Regression (LR), Deep Learning (DL), Generalized Linear Model (GLM), and Support Vector Machine (SVM).

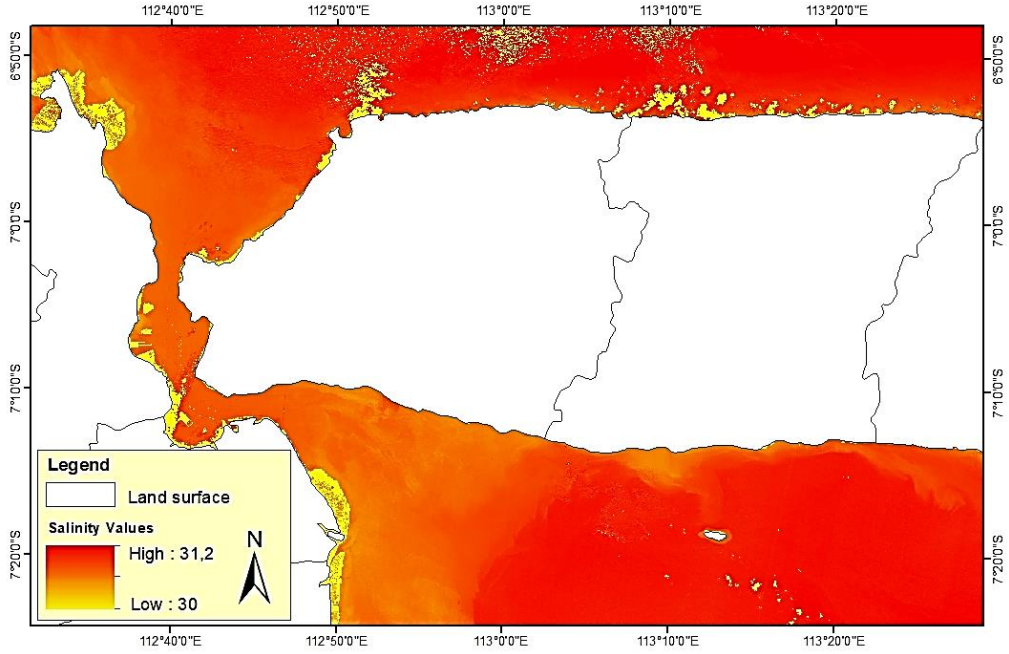

Figure 8. The distribution map of SSS in Madura Strait.

4. Conclusions

The resulting algorithm model is $10^{[-0.0092\times(log_{10}(Kd))+1.4903]}$ Where -0.0092 and 1.4903 were the coefficient and the constant, respectively. The development of an algorithm model to estimate the Sea Surface Salinity (SSS) in Madura strait produced a high accuracy. The indication can be clearly seen in the average difference of the salinity estimation results with the in-situ salinity value, which was very small, 0.0047; in other words, the NMAE value was just 0.47%, while the RMSE value is 0.17. Likewise, when it was applied to the Landsat 8 OLI images, the average difference between the estimated SSS and the in-situ SSS reached an NMAE of 0.51%, while the RMSE value was 0.19. Thus, this model can be used by researchers or practitioners for the needs of sea surface salinity extraction.

Acknowledgements

We are thankful for the Indonesian National Institute of Aeronautics and Space for the supporting in-field campaign**.**

Author Contributions

Conceptualization: Muhsi Muhsi, Bangun Muljo Sukojo, Muhammad Taufik, Pujo Aji, Lalu Muhamad Jaelani; **methodology**: Muhsi Muhsi, Bangun Muljo Sukojo, Muhammad Taufik, Pujo Aji, Lalu Muhamad Jaelani; **investigation**: Muhsi Muhsi; **writing—original draft preparation**: Muhsi Muhsi; **writing—review and editing**: Muhsi Muhsi, Bangun Muljo Sukojo, Muhammad Taufik, Pujo Aji, Lalu Muhamad Jaelani; **visualization**: Muhsi Muhsi. All authors have read and agreed to the published version of the manuscript.

References

Abe, H., Nomura, D., & Hirawake, T. (2021). Salinity regime of the northwestern Bering Sea shelf. *Progress in Oceanography*, *198*. https://doi.org/10.1016/j.pocean.2021.102675

Ahn., Y. H., Shanmugam, P., Moon, J. E., & Ryu, J. H. (2008). Satellite remote sensing of a low-salinity water plume in the East China Sea. *Annales Geophysicae*, *26*(7), 2019–2035.

Akhter, S., Qiao, F., Wu, K., Yin, X., Chowdhury, K. M. A., & Chowdhury, N. U. M. K. (2021). Seasonal and long-term sea-level variations and their forcing factors in the northern Bay of Bengal: A statistical analysis of temperature, salinity, wind stress curl, and regional climate index data. *Dynamics of Atmospheres and Oceans*, *95*. https://doi.org/10.1016/j.dynatmoce.2021.101239

Austin, R. W., & Petzold, T. J. (1981). The Determination of the Diffuse Attenuation Coefficient of Sea Water Using the Coastal Zone Color Scanner. *Marine Science Springer, Boston, MA*, *13*, 239–256.

Austin, R. W., & Petzold, T. J. (1986). Spectral dependence of the diffuse attenuation coefficient of light in ocean waters. *Opt. Eng*, *25*, 473–479.

Bai, Y., Pan, D., Cai, W., He, X., Wang, D., & Tao, B. (2013). Remote sensing of salinity from satellite-derived CDOM in the Changjiang River dominated East China Sea. *Journal Of Geophysical Research: Oceans*, *118*, 227–243. https://doi.org/10.1029/2012JC008467

Binding, CE., & Bowers, DG. (2003). Measuring the salinity of the Clyde Sea from remotely sensed ocean color. *Estuarine, Coastal and Shelf Science*, *57*, 605–611.
Budhiman, S. (2012). Perbandingan Karakteristik Spektral (Spectral Signature) Parameter Kualitas Perairan Pada Kanal Landsat ETM + dan Envisat Meris (Comparion of Water Constituents Spectral Signature on Landsat ETM+ and Envisat Meris Band. *Jurnal Pengideraan Jauh*, *9*(2), 76–89.
Budhiman, S., Suhyb, M., Vekerdy, Z., & Verhoef, W. (2012). Deriving optical properties of Mahakam Delta coastal waters , Indonesia using in situ measurements and ocean color model inversion. *ISPRS Journal of Photogrammetry and Remote Sensing*, *68*, 157–169. https://doi.org/10.1016/j.isprsjprs.2012.01.008
Cuthbert, R. N., Sidow, A., Frost, K. F., Kotronaki, S. G., & Briski, E. (2021). Emergent effects of temperature and salinity on mortality of a key herbivore. *Journal of Sea Research*, *177*. https://doi.org/10.1016/j.seares.2021.102126
Elkhrachy, I. (2021). Accuracy Assessment of Low-Cost Unmanned Aerial Vehicle (UAV) Photogrammetry. *Alexandria Engineering Journal*, *60*(6), 5579–5590. https://doi.org/10.1016/j.aej.2021.04.011
English, S. A., Wilkinson, C., & Baker, V. J. (1997). *Survey Manual For Tropical Marine Resources* (S. A. English, C. Wilkinson, & V. J. Baker, Eds.; second). Australian Institut of Marine Science.
George, J. (2005). *Fundamentals of Remote Sensing* (Second Edi). Universities Press (India).
Gordon, H., Brown, J. W., Evans, R. H., Smith, R. C., Gordon, R., Brown, O. B., Evans, H., Brown, W., & Baker, K. (1988). *A semianalytic radiance model of ocean color*. *July 2014*. https://doi.org/10.1029/JD093iD09p10909
Hair, J. F., W.C., B., B.J., B., R.E., A., & R.L., T. (2006). *Multivariate Data Analysis* (6th ed.).
Hecth, E., Coffey, M., & Dolan, P. (2002). *OPTICS Fourth Edition* (4th ed.). Addison Wesley.
Jaelani, L. M. L. M., Matsushita, B., Yang, W., & Fukushima, T. (2013). Evaluation of four MERIS atmospheric correction algorithms in Lake Kasumigaura, Japan. *International Journal of Remote Sensing*, *34*(24), 8967–8985. https://doi.org/10.1080/01431161.2013.860660
Jaelani, L. M., Limehuwey, R., Kurniadin, N., Pamungkas, A., Koenhardono, E. S., & Sulisetyono, A. (2016). Estimation of Total Suspended Sediment and Chlorophyll-A Concentration from Landsat 8-Oli: The Effect of Atmospher and Retrieval Algorithm. *IPTEK The Journal for Technology and Science*, *27*(1), 16–23. https://doi.org/10.12962/j20882033.v27i1.1217
Jaelani, L. M., Matsushita, B., Yang, W., & Fukushima, T. (2015). An improved atmospheric correction algorithm for applying MERIS data to very turbid inland waters. *International Journal of Applied Earth Observation and Geoinformation*, *39*, 128–141. https://doi.org/10.1016/j.jag.2015.03.004
Lee, Z., & Carder, K. L. (2005a). Diffuse Attenuation Coefficient of Downwelling Irradiance : An Evaluation of Remote Sensing Methods. *Journal of Geophysical Research*, *110*(10).
Lee, Z., & Carder, K. L. (2005b). Diffuse Attenuation Coefficient of Downwelling Irradiance : An Evaluation of Remote Sensing Methods. *Journal of Geophysical Research*, *110*(10).
Lee, Z., Carder, K. L., & Arnone, R. a. (2002). Deriving inherent optical properties from water color: a multiband quasi-analytical algorithm for optically deep waters. *Applied Optics*, *41*(27), 5755–5772.
Lee, Z., Du, K., & Arnone, R. (2005). A model for the diffuse attenuation coefficient of downwelling irradiance. *Journal of Geophysical Research*, *110*(C2), 1–25. https://doi.org/10.1029/2004JC002275
Liemohn, M. W., Shane, A. D., Azari, A. R., Petersen, A. K., Swiger, B. M., & Mukhopadhyay, A. (2021). RMSE is not enough: Guidelines to robust data-model comparisons for magnetospheric physics. *Journal of Atmospheric and Solar-Terrestrial Physics*, *218*. https://doi.org/10.1016/j.jastp.2021.105624
Lillesand, T. M. K. M., Kiefer, R. W., & Chipman, J. (2004). *Remote Sensing and Image Interpretation* (5th ed.). John Wiley {&} Sons, Inc.
Liu, Y., Islam, M. A., & Gao, J. (2003). Quantification of shallow water quality parameters by means of remote sensing. *Progress in Physical Geography*, *27*(1), 24–43. https://doi.org/10.1191/0309133303pp357ra
Lobban, C. S., & Harrison, P. J. (1997). *Seaweed Ecology and Physiology*. Cambridge University Press.
Mobley, C. D. (1999a). Estimation of Remote Sensing Reflectance from Above-Surface Measurements. *Applied Optics*, *38*(36), 7442–7455.
Mobley, C. D. (1999b). Estimation of the remote-sensing reflectance from above-surface measurements. *Applied Optics*, *38*(36), 7442–7455.
Morel, A. (1988). Optical modeling of the upper ocean in relation to its biogenous matter content (case 1 waters). *J. Geophys. Res*, *93*, 10749– 10768.
Morel, A., & Maritorena, S. (2001). Bio-optical properties of oceanic waters: A reappraisal. *J. Geophys. Res*, *106*, 7163–7180.
Muhsi, M., Sukojo, B. M., Taufik, M., & Aji, P. (2017). Model Pendugaan Kandungan Sulfat di Air Laut Menggunakan Citra Satelit Landsat 8 OLI. *Konferensi Nasional Teknik Sipil Dan Infrastruktur*, 13–22.
Muhsi, M., Sukojo, B. M., Taufik, M., & Aji, P. (2018). Estimation Algorithm of Sulfate Concentration at The Sea Surface Based on Landsat 8 OLI Data. *Journal of Theoretical and Applied Information Technology*, *96*(17), 5741–5753.
Muhsi, M., Sukojo, B. M., Taufik, M., & Aji, P. (2020). Mapping and Analysis A Distribution of Sulfate Concentration at The Sea Surface of Madura Strait Using Geographic Information System (GIS) Based on Landsat 8 OLI Data. *IOP Conference Series: Earth and Environmental Science*, *469*(1), 12090. https://doi.org/10.1088/1755-1315/469/1/012090
Nababan, B., Wirapramana, A. A., & Arhatin, R. E. (2013). Spectral of Remote Sensing Reflectance of Surface Waters. *Jurnal Ilmu Dan Teknologi Kelautan Tropis*, *5*(1), 69–84.
Nafizah, Jaelani, L. M., & Winarso, G. (2016). Evaluasi Algoritma Wouthuyzen dan Son untuk Pendugaan Sea Surface Salinity (SSS) (Studi Kasus: Perairan Utara Pamekasan). *Jurnal Teknik ITS*, *5*(September).
Nybakken, James W. (2001). *Marine Biology : An Ecological Approach* (5th ed.). Benjamin-Cummings Publishing Company.
Salim, D., Yuliyanto, & Baharuddin. (2017). Karakteristik Parameter Oseanografi Fisika-Kimia Perairan Pulau Kerumputan Kabupaten Kotabaru Kalimantan Selatan. *Enggano*, *2*(2), 218–228.
Sasaki, H., Siswanto, E., Nishiuchi, K., Tanaka, K., & Hasegawa, T. (2008). Mapping the low salinity Changjiang Diluted Water using satellite- retrieved colored dissolved organic matter (CDOM) in the East China Sea during high river flow season. *Geophysical Research Letters*, *35*, 1–6. https://doi.org/10.1029/2007GL032637
Scale, S. (2009). *Satellite Remote Sensing : Salinity Measurements*. 127–132.
Son, Y. B., Gardner, W. D., Richardson, M. J., Ishizaka, J., Ryu, J.-H., Kim, S.-H., & Lee, S. H. (2012). Tracing offshore low-salinity plumes in the Northeastern Gulf of Mexico during the summer season by use of multispectral remote-sensing data. *Journal of Oceanography*, *68*(5), 743–760. https://doi.org/10.1007/s10872-012-0131-y
Wang, F., & Xu, Y. J. (2008). *Development and application of a remote sensing-based salinity prediction model for a large estuarine lake in the US Gulf of Mexico coast*. 184–194. https://doi.org/10.1016/j.jhydrol.2008.07.036

Wei, J., & Lee, Z. (2013a). Model of the attenuation coefficient of daily photosynthetically available radiation in the upper ocean. *Methods in Oceanography*, *8*, 56–74. https://doi.org/10.1016/j.mio.2013.12.001

Wei, J., & Lee, Z. (2013b). Model of the attenuation coefficient of daily photosynthetically available radiation in the upper ocean. *Methods in Oceanography*, *8*, 56–74. https://doi.org/10.1016/j.mio.2013.12.001

Wouthuyzen, S., Tarigan, S., Indarto, H., Supriyadi, Sediadi, A., Sugarin, Siregar, V. P., & Ishizaka, J. (2008). Pengukuran Salinitas Permukaan Teluk JakartaMelalui Penginderaan Warna Laut MenggunakanData Multi-Temporal Citra Satelit Landsat-7 ETM+. *PIT MAPIN XVII*.